Proceeding of the 2004 American Control Conference
Boston, Massachusetts June 30 - July 2, 2004

Semi-Active Vibration Control Using Piezoelectric-Based Switched Stiffness

Arun Ramaratnam[1], Nader Jalili[1*] and Darren M. Dawson[2]
Smart Structures and Nanoelectromechanical Systems Laboratory,
Clemson University, Clemson, South Carolina 29634, U.S.A.

***Abstract* — A switched stiffness semi-active vibration attenuation method implemented with a simple relay-type control logic for flexible mechanical structures is presented. A single degree of freedom system is considered for validation of the switched stiffness concept. The method is then applied to a flexible beam with moving base, representing the last link of a Cartesian-type robot manipulator. A piezoelectric actuator, attached on the top surface of the flexible beam, is switched between open and short circuit configurations. This switching introduces a change in stiffness, which, in turn, can remove energy from the overall system by directly affecting the stored potential energy in the flexible beam. The control logic for switching stiffness is based on the position and velocity feedback of the tip of the flexible beam. Implementation of this control logic is hindered by the lack of velocity sensors. A numerical differentiator may be utilized, but may degrade the vibration suppression performance due to the phase lag introduced by filters utilized for conditioning the resultant noisy signal. In order to remedy this, a novel output feedback variable structure velocity observer scheme applicable for a general nonlinear mechanical system with unknown system dynamics is utilized. Simulation results show superior vibration attenuation for both the single degree of freedom oscillator and the cantilever flexible beam systems with velocity observer.**

1. Introduction

Piezoelectric materials have been used in the past as actuators and sensors in active and passive vibration control of dynamic structures. Active vibration control methods, though effective in vibration attenuation, require large amounts of input energy and may cause instability under certain conditions [1]. Passive vibration control methods, on the other hand, are less effective in vibration control but are relatively simpler and have much improved stability characteristics compared to active systems [1]. Passive vibration control using piezoelectric materials also suffer from many drawbacks such as detuning modes, large inductance requirements for low excitation frequencies, and limitations on electromechanical coupling potential of the piezoelectric elements. There is always a trade-off between active and passive vibration control methods, which has led to the development of hybrid methods such as adaptive passive and semi-active configurations [2, 3].

[1]Dept. of Mechanical Engineering, [2]Dept. of Electrical and Computer Engineering, *Corresponding Author, Email: jalili@clemson.edu.

A recent development in this area utilizes piezoelectric actuators with switched stiffness [4, 5]. The switched stiffness method is a semi-active vibration control method in which a control law is designed to switch the equivalent stiffness effect of the piezoelectric actuator. This is primarily based on the property of the piezoelectric materials that results in a significant change in the mechanical stiffness of the combined system between open circuit and short circuit configurations [4]. In this method, a piezoelectric actuator is switched between high stiffness (in the form of an open circuit) and low stiffness (in the form of a closed circuit), in order to increase the energy dissipated from the system.

The high stiffness state is used when the system is moving away from its equilibrium point such that potential energy is stored in the bending or deflection of the system. The piezoelectric actuator is switched to low stiffness state when the system has reached its maximum stored potential energy, thus dissipating energy by lowering the stiffness. This energy dissipating method can be used for vibration suppression of transient and continuously excited systems. However, a limitation for implementation of this type of vibration attenuation is the velocity measurement requirement of the system under study. Expensive velocity sensors and noisy differentiators make this limitation more noticeable. This problem can be overcome by implementing an output feedback velocity observer [6].

Typically, embedded piezoelectric actuators serve as non-collocated controllers for vibration suppression requirements [7-12]. To predict the behavior of the flexible beams incorporating PZT actuators and sensors, many exact (analytical) and approximate (numerical) models have been developed [13-16]. These mathematical models consider the piezoelectric patches in the form of either bonded on the transverse surface or embedded in the beam, and assume linear strain in the actuator and a pure shear in the bond film [14-16].

In this paper, a switched stiffness control strategy is proposed for regulating a single link robot arm, which is modeled as a flexible cantilever beam with a translational base support. The base motion is excited by utilizing an electrodynamic shaker, while a PZT patch actuator is bonded on the surface of the flexible beam for suppressing

0-7803-8335-4/04/$17.00 ©2004 AACC

residual arm vibrations. The control objective here is to suppress the vibration transients in the beam in the presence of base motion and disturbances. The controller developed here is a semi-active controller using stiffness switching. The velocity of the robot arm is estimated using an observer using output feedback variable structure observer [6]. The results obtained by varying the stiffness demonstrate that the beam residual vibrations can be suppressed to achieve stable performance of the robot arm.

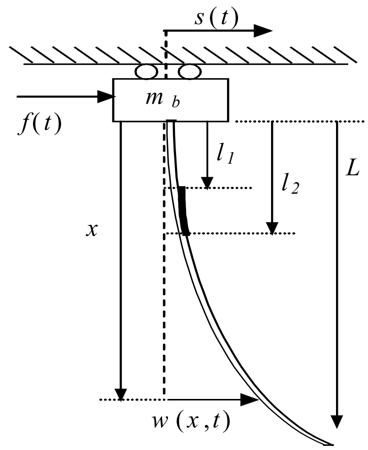

Figure 1: Schematic of a one-link flexible robot arm.

2. Governing Equations of Motion

As shown in Figure 1, one end of the beam is clamped into a moving base with the mass of m_b, while the other end is free. The beam has total thickness t_b, and length L, and the piezoelectric film possesses thickness and length of t_b and (l_2-l_1), respectively. We assume that the PZT and the beam have the same width, b. The PZT actuator is perfectly bonded on the beam at distance l_1, measured from the beam support. The force $f(t)$ acting on the base is the only external effect.

Uniform cross-section with Euler-Bernoulli beam assumptions is considered for the beam. It is assumed that there is no axial deformation for the beam and the small deflection assumption is satisfied. If $s(t)$ is the base displacement, $w(t)$, the beam tip displacement, ρ_b and ρ_p, respective beam and PZT volumetric densities, E^b and E^p represent the young's modulus of the beam and the PZT, neglecting the effect of gravity, the equations of motion can be obtained as in [17],

$$m_b\ddot{s}(t)+\int_0^L \rho(x)\big(\ddot{s}(t)+\ddot{w}(x,t)\big)dx = f(t) \quad (1)$$

$$\rho(x)\big(\ddot{s}(t)+\ddot{w}(x,t)\big)+\frac{\partial^2}{\partial x^2}\big(EI(x)w''(x,t)\big)=0 \quad (2)$$

with the boundary conditions

$$w(0,t)=0\,,\ w'(0,t)=0\,,\ w''(L,t)=0\,,\ w'''(L,t)=0 \quad (3)$$

where

$$\rho(x)=(\rho_b t_b + S(x)\rho_p t_p)b \quad (4)$$

$$EI(x)=EI^b+EI^pS(x) \quad (5)$$

$$EI^b=\frac{bE^bt_b^3}{12} \quad (6)$$

$$EI^p=bE^pt_p\left\{\frac{t_b^2}{4}+\frac{t_bt_p}{2}+\frac{t_p^2}{3}-\frac{z_n}{2}(t_b+t_p)\right\} \quad (7)$$

$$S(x)=H(x-x_1)-H(x-x_2) \quad (8)$$

and $H(x)$ is the Heaviside function. Considering the system's governing equations (1-3), the modulus of elasticity of the PZT, EI^p given in equation (7), can be varied by switching the circuit connection of the shunted piezoelectric between open and short circuit configurations. Notice the switched stiffness method is a semi-active method and the piezoelectric actuator attached to the beam acts as energy dissipating mechanism rather than an active control system. When short-circuited, the modulus of elasticity is EI^p, while in open circuit, it is $EI^p/(1-k_{31}^2)$, thereby introducing a change in stiffness (this will be demonstrated later in the text), where k_{31} is the electromechanical coupling coefficient. The benefit of changing stiffness is shown in Section 3 followed by the switched stiffness proposition using PZT actuators in Section 5.

3. Switched Stiffness Vibration Control Concept

To best explain the switched stiffness vibration control method, we consider a single-degree-of-freedom (SDOF) mass-spring system. The spring is assumed to be a step-variable stiffness spring in the sense that it can be switched between two constant values, namely high and low stiffness values. As the external force $f(t)$ causes the mass to move away from its equilibrium position, the stiffness of the spring $k(t)$ is kept at high value. The maximum potential energy at maximum mass displacement will be given by $\frac{1}{2}k_{high}y_{\max}^2$. At this point ($y_{max}$), the stiffness is switched to low value and kept at this value until the mass reaches the equilibrium point again. Therefore, the potential energy at y_{max} becomes $\frac{1}{2}k_{low}y_{\max}^2$. The difference in potential energy can be given as $\frac{1}{2}\Delta k\, y_{\max}^2$. The decrease in potential energy given by $\frac{1}{2}\Delta k\, y_{\max}^2$ will consequently result in decrease in converted kinetic energy, thereby introducing energy dissipation in the system. The stiffness is then switched back to high when the system moves away from its equilibrium, thus switching stiffness from low to high in a periodic manner to gradually dissipate system energy.

3.1 Control Law for Switching Stiffness

A heuristic control law was suggested in [4] to essentially switch the stiffness values through a hard switching or on-off (relay) control. For the case of the SDOF system discussed in Section 3, the governing equation of the system is given by

$$m\ddot{y}(t)+k(t)y(t)=f(t) \tag{9}$$

where y is the system output (i.e., the signal that is to be attenuated). The control law can be simply stated as

$$\begin{cases} k(t) &= k_{high} \quad \text{for } y\dot{y}\geq 0 \\ k(t) &= k_{low} \quad \text{for } y\dot{y}<0 \end{cases} \tag{10}$$

The control law can also be expressed in the following more compact form,

$$k(t)=\frac{(1+\operatorname{sgn}(y\dot{y}))}{2}(k_{high}-k_{low})+k_{low} \tag{11}$$

For numerical simulations, the spring stiffness value is changed such that the potential energy is dissipated at maximum deflection, resulting in the 'step-down' of total system energy, and hence, suppressing the displacement as shown in the bottom graph of Figure 2. The amount of dissipated energy over a particular period is proportional to the difference between high and low values (Δk as explained earlier in this section). When the stiffness is switched as per control law given in equation (10), it results in significant vibration suppression [5]. Note that the system is no more conservative, due to the dependence of the stiffness with time, hence it is considered as a parametric system.

3.2 Lyapunov-based Stability Analysis of Switched Stiffness Method

Theorem 1: The homogenous version (*f(t)* = 0) of the quasi time-variant linear system (equation (9)) with the variable-rate stiffness *k(t)* given by equation (11) is globally asymptotically stable in the sense that $y(t)\to 0$ as $t\to\infty$.

Proof: We select a Lyapunov candidate function,

$$V=\frac{1}{2}m\dot{y}^2+\frac{1}{4}(k_{high}+k_{low})y^2 \tag{12}$$

We see that V is positive definite. Differentiating equation (12), and using equation (9), it can be shown that,

$$\dot{V}=-\frac{1}{2}(k_{high}-k_{low})\left|y\dot{y}\right| \tag{13}$$

Considering that $\dot{V}$ is negative semi-definite, V is radially unbounded, i.e. $V\to\infty$, as $\|y\|\to\infty$, then, using the Invariant Set Theorem [18], it can be proven that the system (9) with variable spring (*k(t)*) is globally asymptotically stable. The phase portrait shown in Figure 3 demonstrates that the switched stiffness system results in a globally asymptotically stable equilibrium point.

4. Real Time Implementation of Switched Stiffness Concept using Velocity Observer

The control law can be implemented by measuring the position and the velocity of the spring-mass system, but due to the unavailability (or complication of implementation) of velocity sensors, velocity cannot be measured directly, thus hindering the implementation of the control law. In order to overcome this dilemma, a simple solution would be to measure the position and numerically differentiate it to find the required velocity signal. A classical problem is the resulting noise accompanying the differentiated signal leading to erroneous results. To prevent this, a recent robust velocity observer scheme can be utilized to observe the velocity and help implement the control law [6]. This observer may also be considered as an inexpensive replacement for the velocity sensors.

Velocity Observer Design Overview: This section briefly explains the variable structure velocity observer introduced in [6] for a class of unknown nonlinear systems of the form

$$\ddot{y}=h(y,\dot{y})+G(y,\dot{y})u \tag{14}$$

where $y(t)\in\Re^n$ is the system output, $u(t)\in\Re^n$ is the system input, $h(y,\dot{y})\in\Re^n$ and $G(y,\dot{y})\in\Re^n$ are system nonlinear functions. The following assumptions are made in order to design the observer [6]:

1. The system states are always bounded.
2. $h(y,\dot{y})$ and $G(y,\dot{y})$ are first order differentiable such that their derivatives exist.
3. The control input $u(t)$ is first order differentiable.

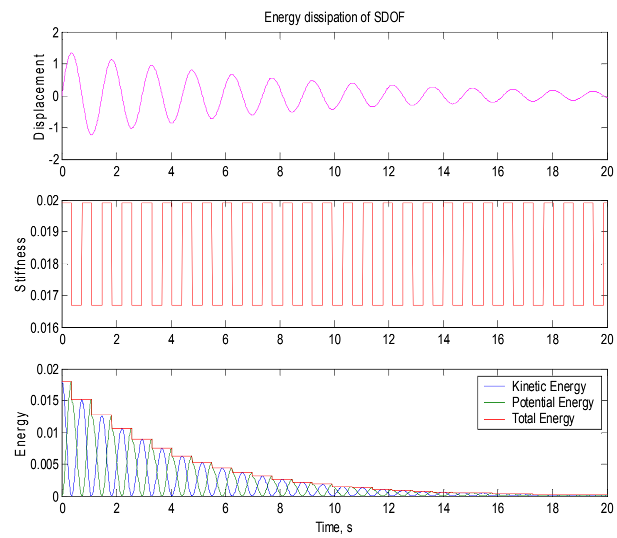

Figure 2: Illustration of the stiffness switching concept for a SDOF system with *m* = 1 *g*, k_{low} = 16.7 *kg/mm* and k_{high} = 19.9 *kg/mm*.

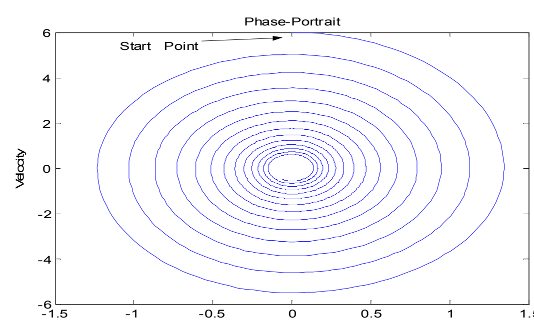

Figure 3: Phase portrait of the variable spring-mass system indicating asymptotic stability.

If $\hat{\dot{y}}(t)$ is the observed velocity, then the error due to the velocity observation can be given as,

$$\tilde{\dot{y}} = \dot{y} - \hat{\dot{y}} \tag{15}$$

Therefore, to observe velocity accurately, the error should go to zero, $\tilde{\dot{y}} \to 0$, as $t \to \infty$. In order to achieve this, a second-order filter, whose structure is motivated by the Lyapunov-type stability analysis as in [6], is adopted as follows to generate the needed velocity,

$$\hat{\dot{y}} = p + K_0 \tilde{y} \tag{16}$$

$$\dot{p} = K_1 \operatorname{sgn}(\tilde{y}) + K_2 \tilde{y} \tag{17}$$

where $p(t)$ is an auxiliary variable, sgn(.) denotes the standard signum function, K_0, K_1 and K_2 are positive-definite constant diagonal matrices. The stability analysis has also been proven in [6], ensuring stability of the system using this observer.

The switched stiffness control concept is implemented using the position and the estimated velocity via the output feedback observer explained earlier. The SDOF system in section 3 is considered with the velocity observer presented in the above section for the simulation. Appropriate gains K_0, K_1 and K_2 were selected and the results are obtained as shown in Figure 4. The velocity observation error goes to zero as seen in the third graph of Figure 4, as a result of which the observed velocity corresponds to the actual velocity as shown in the last two graphs of Figure 4.

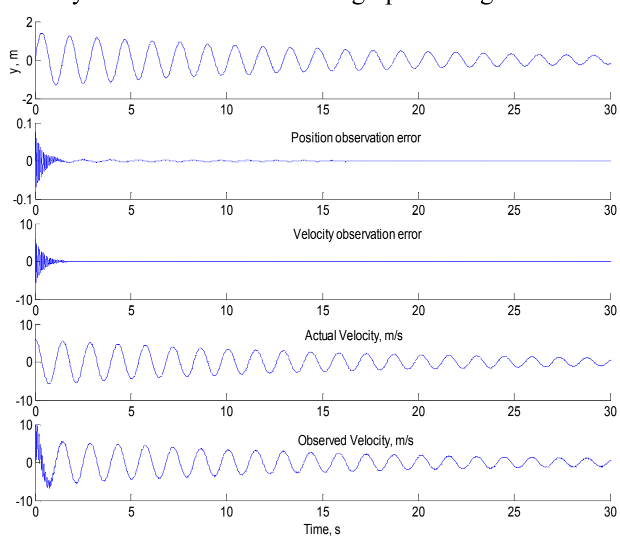

Figure 4: Velocity observer performance for switched stiffness SDOF system with gains K_0 = 5, K_1 = 5 and K_2 = 5500.

5. Switched Stiffness using PZT Actuators

The switched-stiffness method utilizing a variable stiffness spring was explained earlier. This section presents the practical implementation of such concept through utilization of piezoelectric patch actuators. The piezoelectric materials possess the ability to change the effective stiffness according to the type of circuit connection [4]. More specifically, when connected in an open circuit, the material exhibits a particular stiffness and when short-circuited, it exhibits different, typically lower stiffness. This ability of the piezoelectric actuators to change their stiffness is due to their ability to change their mechanical compliance, caused by changes in their electrical impedance when connected in open or short circuit.

During open circuit, the piezoelectric actuator is able to store more potential energy due to its higher stiffness and inherent capacitance, when switched to low stiffness (i.e. short circuit), the piezoelectric is able to dissipate the energy effectively as the capacitor is shunted to short and the stiffness becomes low. If the piezoelectric actuator is shunted to a resistive (R) or resistive-inductive (R-L) circuit, the resistor dissipates electrical energy in the form of heat energy [1]. Passively shunted systems provide better performance than the simple open-closed type systems; however, they tend to show inconsistency and poor performance if not optimally tuned.

There are two basic theories on the utilization of piezoelectric patch actuators as vibration controller. The first theory regards the actuator as an added viscous spring damper where the piezoelectric has a particular value of stiffness. The second theory concentrates on energy conversion approach, where mechanical energy is converted into electrical energy, through the inherent electromechanical coupling of the piezoelectric actuator, which in turn is dissipated. The piezoelectric actuator acts like a voltage source with a capacitor in the circuit. To use the basic concepts of admittance and impedance, we can write voltage and current across the piezoelectric actuator as in [1],

$$v(s) = L\,\mathbf{E}(s) \tag{18}$$

$$I(s) = s\,A\,\mathbf{D}(s) \tag{19}$$

where $\mathbf{E}$ is the electrical field of the PZT and $\mathbf{D}$ is the dielectric displacement of the PZT. v is the voltage of the piezoelectric actuator, I is the current flowing through the actuator, A is the cross sectional area of the actuator and L is the length of the piezoelectric actuator. Now the stress and strain can be written with respect to voltage and current as [1],

$$\begin{bmatrix} \mathbf{I} \\ \mathbf{S} \end{bmatrix} = \begin{bmatrix} sA\boldsymbol{\varepsilon}_{33}L^{-1} & sA\mathbf{d}_{31} \\ \mathbf{d}_{31}L^{-1} & \mathbf{s}^{\mathbf{E}} \end{bmatrix} \begin{bmatrix} \mathbf{V} \\ \mathbf{T} \end{bmatrix} \tag{20}$$

where $\mathbf{s}^{\mathrm{E}} \in \Re^{6\times6}$ refers to the compliance of material when the electric field is constant, $\boldsymbol{\varepsilon}^{\mathrm{T}} \in \Re^{3\times3}$ is the permittivity matrix under constant stress and $\mathbf{d}$ relates the electric charge per unit area $\mathbf{D} \in \Re^{3}$ (the dielectric displacement) to the stress $\mathbf{T}$ under a zero electric field. On the other hand, we can write

$$A\boldsymbol{\varepsilon}_{33}L^{-1} = C_{pzt} \tag{21}$$

where C_{pzt} is the capacitance of the piezoelectric actuator.

5464

Replacing the inherent capacitance of the piezoelectric actuator with open circuit admittance $Y^D(s)$ of the piezoelectric actuator in equation (20) we get,

$$\begin{bmatrix}\mathbf{I}\\ \mathbf{S}\end{bmatrix}=\begin{bmatrix}Y^D(s) & sA\mathbf{d}_{31}\\ \mathbf{d}_{31}L^{-1} & \mathbf{s}^{\mathbf{E}}\end{bmatrix}\begin{bmatrix}\mathbf{V}\\ \mathbf{T}\end{bmatrix} \tag{22}$$

Expressing equation (22) in terms of electrical impedance Z^{EL}, which is the reciprocal of electrical admittance, Y^D, we arrive at the voltage appearing across the piezoelectric actuator electrodes,

$$v = Z^{EL}I-(Z^{EL}sAD)T \tag{23}$$

The ability of the piezoelectric actuator to change the stiffness according to its circuit connection is noted by the fact that the mechanical compliance, the reciprocal of stiffness changes accordingly for different circuit connections. The shunted piezoelectric compliance can be defined [1] by

$$s^{SU} = [s^E - sAd_{31}^2L^{-1}Z^{EL}] \tag{24}$$

For open circuit, we have

$$Z^{EL} = (C_{pzt}s)^{-1} \tag{25}$$

while for short circuit, we get

$$Z^{EL} = 0 \tag{26}$$

If a shunt circuit is used, then Y^D is replaced by Y^{EL}, and if Z^{sh} is the shunt circuit impedance, then:

$$Y^{EL} = Y^D + Y^S \tag{27}$$

$$Z^{EL} = (C_{pzt}s)^{-1} + Z^{sh} \tag{28}$$

By using different values for Z^{EL}, the piezoelectric compliance changes, thus implying change in stiffness. It is evident that the open circuit compliance is less than that of short circuit, implying that the open circuit stiffness is higher than short circuit. In case of shunted piezoelectric, greater the impedance of the shunt circuit greater will be the stiffness of the piezoelectric actuator.

The electromechanical coupling coefficient is defined as the ratio of the peak energy stored in the capacitor to the peak energy stored in the material strain (under uniaxial loading and sinusoidal motion) with the piezoelectric electrodes open. Physically, its square represents the percentage of mechanical strain energy, which is converted into electrical energy and vice-versa. The electromechanical coupling coefficient is defined as [19]

$$k_{31}^2 = \frac{E^P d_{31}^2}{\varepsilon_{33}} \tag{29}$$

where E^P is the equivalent stiffness of the PZT. This implies from equations (24), (25), (26) and (29) that the change in stiffness will be from a low stiffness value $E^P{}_{low} = E^P = (s^E)^{-1}$ to a high equivalent stiffness value of $E^P{}_{high} = E^P/(1-k_{31}^2)$.

6. Switched Stiffness Method for Translational Flexible Beams

A flexible translational Cartesian robot can be modeled as a flexible cantilever beam with a translational base support (Figure 1). The effectiveness of the switched stiffness method is demonstrated here by implementing it on the flexible cantilever beam arm with a translational base support shown in Figure 1.

6.1 Assumed Mode Model Expansion

For the numerical simulations, an assumed mode model (AMM) expansion is used to truncate the original partial differential equations. Specifically, the beam deflection *w(x,t)* is expressed as the following Galerkin approximate:

$$\begin{aligned} w(x,t) &= \sum_{i=1}^{n}\phi_i(x)q_i(t) \\ P(x,t) &= s(t)+w(x,t) \end{aligned} \tag{30}$$

where $\phi_i(x)$'s are the mode shapes of the flexible cantilever beam, $q_i(t)$'s are the generalized coordinates and n is the number of modes to be considered. Using Lagrangian approach and utilizing standard orthogonality conditions for the mode shapes, the equations of motion can be obtained as [17, 20- 21]

$$m_i\ddot{s}(t) + m_{di}\ddot{q}_i(t) + \omega_i^2 m_{di}q_i(t) = 0 \quad , \; i = 1,2,...,n \tag{31}$$

$$[m_b + \int_0^L \rho(x)dx]\ddot{s}(t) + \sum_{j=1}^{\infty} m_j\ddot{q}_j(t) = f(t) \tag{32}$$

where,

$$\begin{aligned} m_i &= \int_0^L \rho(x)\phi_i(x)\,dx \\ m_{di} &= \int_0^L \rho(x)\phi_i^2(x)\,dx \end{aligned} \tag{33}$$

and ω_i's are natural frequencies of the beam.

6.2 Switched Stiffness Control Implementation

As stated earlier, the objective here is to suppress the vibrations of the robot arm through the switched-stiffness method while the arm base undergoes external motion. Similar to the control law in Section 3 for the SDOF system (see equation (10)), the beam tip deflection, $w(L,t)$ is used as the system output. Consequently, the control law is stated

$$\text{as,}\begin{cases} E^P = E^p/(1-k_{31}^2) & \text{for } w(L,t)\,\dot{w}(L,t) \geq 0 \\ \text{(switch to high stiffness or open circuit)} & \\ E^P = E^p & \text{for } w(L,t)\,\dot{w}(L,t) < 0 \\ \text{(switch to low stiffness or short circuit)} & \end{cases} \tag{34}$$

where $w(L,t)$ and $\dot{w}(L,t)$ correspond to respective y and $\dot{y}$ as in SDOF setting. The change in low stiffness and high stiffness can be performed by changing the value of E^p in equation (5); that is, for low stiffness $E_{low}^p = E^p$ and for high stiffness $E_{high}^p = E^p/(1-k_{31}^2)$.

For numerical simulations, three modes of the flexible beam are considered (n = 3). Viscous and structural damping of the beam are both neglected for simulations. The condition for switching is checked and the control law is implemented as mentioned above (equation (34)), thus switching the piezoelectric actuator from low to high stiffness. The parameters used are listed in [17]. The results are shown in Figure 5, where considerable vibration suppression is noted. Modal velocities obtained by solving the differential equations for the system were used to implement the control law in this simulation, but this is not possible in real time. Many strain sensors are needed to determine the modal velocity and then calculate the beam tip velocity. Hence other means for velocity measurement are required, which are discussed next.

6.3 Switched Stiffness Implementation via Velocity Observer

The flexible beam with moving base is considered here again and the velocity observer developed in Section 4 is used for simulation. Appropriate gains K_0, K_1 and K_2 are selected and the following results are obtained as shown in Figure 6. The results are similar to that obtained in Figure 5, justifying the use of the observer.

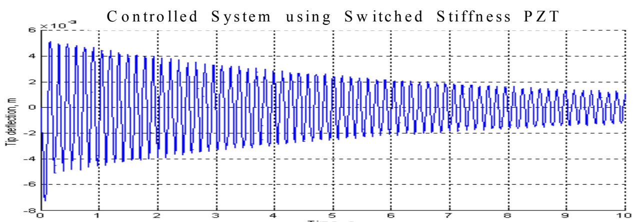

Figure 5: Response of the beam tip deflection for switched stiffness using modal velocities.

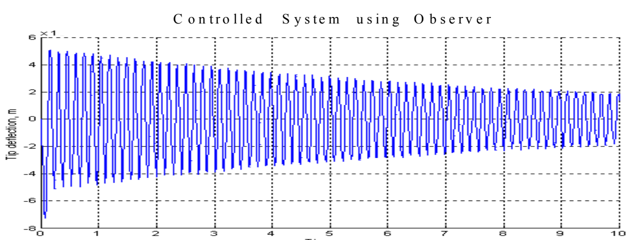

Figure 6: Response of the beam tip deflection for switched stiffness system using velocity observer.

7. CONCLUSIONS

A flexible translational cantilever beam equipped with a piezoelectric actuator attachment that could change its stiffness was considered here. By switching the stiffness, (i.e., PZT configuration) depending on the position of the beam tip with respect to the equilibrium, energy dissipation was maximized and considerable vibration suppression was achieved. Real-time implementation difficulty with regard to velocity measurement was overcome using an output feedback variable structure observer. Experimental validation of the vibration attenuation for flexible beams using switched stiffness technique with the proposed velocity observer is under investigation.

REFERENCES

1. Hagood, N. W. and Von Flotow, A., 1991, "Damping of Structural Vibrations with Piezoelectric Materials and Passive Electrical Networks", *Journal of Sound and Vibration*, **146** (2), pp. 243-268.
2. Jalili, N., 2000, "A New Perspective for Semi-Automated Structural Vibration Control", *Journal of Sound and Vibration,* **238** (3), pp. 481-494.
3. Jalili, N., 2002, "A Comparative Study and Analysis of Semi-Active Vibration-Control Systems", *ASME Journal of Vibration and Acoustics*, **124**, pp. 593-605.
4. Clark, W. W., 2000, "Vibration Control with State-Switched Piezoelectric Materials", *Journal of Intelligent Material Systems and Structures,* **11** (4), pp. 263-271.
5. Ramaratnam, A., Jalili, N., and Grier, M., 2003, "Piezoelectric vibration suppression of translational flexible beams using switched stiffness", *Proc. of 2003 IMECE*, ASME, Washington, D.C.
6. Xian, B., de Queiroz, M. S., Dawson, D. M. and McIntyre, M. L., 2003, "Output Feedback Variable Structure Control of Nonlinear Mechanical Systems", *Proc. of IEEE Conference on Decision and Control,* Hawaii.
7. Crawley, E. F. and Anderson, E. H., 1990, "Detailed Models of Piezoelectric Actuation of Beam", *Journal of Intelligent Material System and Structures*, **1**, pp. 4-25.
8. Gaundenzi, P., Carbonaro, R. and Benzi, E., 2000, "Control of Beam Vibrations by Means of Piezoelectric Devices: Theory and Experiments", *Composite Structures*, **50**, pp. 373-379.
9. Ge, S. S., Lee, T. H. and Gong, J. Q., 1999, "A Robust Distributed Controller of a Single-link SCARA/Cartesian Smart Materials Robot", *Mechatronics*, **9**, pp. 65-93.
10. Jalili, N., Dadfarnia, M., Hong, F. and Ge, S. S., 2002, "An Adaptive Non Model-Based Piezoelectric Control of Flexible Beams with Translational Base", *Proc. of the American Control Conference*, **5**, Anchorage, Alaska, pp. 3802-3807.
11. Oueini, S. S., Nayfeh, A. H., and Pratt, J. R., 1998, "A Nonlinear Vibration Absorber for Flexible Structures", *Nonlinear Dynamics*, **15**, pp. 259-282.
12. Sunar, M., Hyder, S. J. and Yilbas, B. S., 2001, "Robust Design of Piezoelectric Actuator for Structural Control", *Computer Methods in Applied Mechanics and Engineering*, **190**, pp. 6257-6270.
13. Chandrashekhara, K., and Varadarajan, S., 1997, "Adaptive Shape Control of Composite Beams with Piezoelectric Actuators", *Journal of Intelligent Material System and Structures*, **8**, pp. 112-124.
14. Crawley, E. F., and Anderson, E. H., 1990, "Detailed Models of Piezoelectric Actuation of Beam", *Journal of Intelligent Material System and Structures*, **1**, pp. 4-25.
15. Wang, B. T., and Rogers, C. A., 1991, "Laminated Plate Theory for Spatially Distributed Induced Strain Actuators", *Journal of Composite Materials*, **25**, pp. 433-452.
16. Ge, S. S., Lee, T. H., and Gong, J. Q., 1998, "Dynamic Modeling of a Smart Materials Robot", *AIAA Journal*, **36** (8), pp. 1466-1478.
17. Dadfarnia, M., Jalili, N., Xian, B. and Dawson, D. M., 2003, "A Lyapunov-based Piezoelectric Controller for Flexible Cartesian Robot Manipulators", *ASME Journal of Dynamic Systems, Measurements and Control*, in print (June 2004 issue).
18. Slotine, J. J. and Li. W, 1991, "*Applied Nonlinear Control*", Prentice Hall.
19. Lee, T. H., Ge, S. S. and Wang, Z. P., 2001, "Adaptive Robust Controller Design for Multi-Link Flexible Robots", *Mechatronics*, **11** (8), pp. 951-967.
20. Preumont, A., 1997, *Vibration Control of Active Structures: An Introduction*, Kluwer Academic Publishers.
21. Liu, Z., Jalili, N., Dadfarnia, M. and Dawson, D. M, 2002, "Reduced-order Observer based Piezoelectric Control of Flexible Beams with Translational Base", *Proc. of 2002 IMECE*, New Orleans, Louisiana.